10.4 ASSESSING THE FORECAST IMPACTS OF SIMULATED GEMS OBSERVATIONS

Joseph G. Dreher[1], John Manobianco, Randolph J. Evans, and Jonathan L. Case
ENSCO, Inc., Melbourne, FL

1. INTRODUCTION

Technological advancements in Micro Electro Mechanical Systems (MEMS) and nanotechnology have inspired a concept for a revolutionary observing system called Global Environmental Micro Sensors (GEMS). The system features a massive, wireless network of in situ, buoyant airborne probes that can monitor all regions of the Earth with unprecedented spatial and temporal resolution. The probes will be designed to remain suspended in the atmosphere for hours to days and take measurements of temperature, humidity, pressure, and wind velocity that are commonly used as dependent variables in numerical weather prediction (NWP) models. As a result, it will not be necessary to develop complex algorithms for assimilating such data into research or operational models.

In addition to gathering meteorological data, probes could be used for environmental monitoring of particulate emissions, organic and inorganic pollutants, ozone, carbon dioxide, and chemical, biological, or nuclear contaminants. Once the probes settle out of the atmosphere, they could continue making surface measurements over land or water.

This paper provides a discussion of the system used to simulate dispersion of and observations collected by an ensemble of probes. The GEMS simulation system is described in section 2. Section 3 highlights the several possible deployment scenarios and section 4 describes a preliminary set of Observing System Simulation Experiments (OSSEs) performed to assess the forecast impacts of GEMS on NWP models.

2. SIMULATION SYSTEM

The Advanced Regional Prediction System (ARPS; Xue et al. 2000; Xue et al. 2001) coupled with a Lagrangian particle model (LPM) is used to simulate the dispersion of observations collected by an ensemble of probes. The ARPS is a complete, fully automated, stand-alone system designed to forecast explicitly storm- and regional-scale weather phenomena. It includes a data ingest, quality control, and objective analysis package known as ADAS (ARPS Data Analysis System; Brewster 1996), a prediction model, and a post-processing package.

Probe dispersion is simulated using the LPM embedded within ARPS. The probes are assumed to be passive tracers moving independent of one another and transported by the wind. The LPM tracks the location of each probe based on three-dimensional wind components and updates probe position using the resolvable-scale components of wind velocity directly from the ARPS model, as well as turbulent velocity fluctuations. The turbulent velocity fluctuations are estimated from a subgrid scale (SGS) turbulence parameterization (Mellor and Yamada 1980) similar to the SGS turbulence scheme of Deardorff (1980) used in the ARPS model. A parameterization scheme for wet deposition or precipitation scavenging is included in the LPM to simulate the impact of frozen and liquid precipitation on probe trajectory and possible washout (Seinfield and Pandis 1998).

3. DEPLOYMENT SCENARIOS

A large number ($>10^6$) of simulated probes can be deployed at any time during the model integration, and at any latitude, longitude, and altitude within the three-dimensional ARPS domain. The LPM provides accurate position information because the velocity variables are updated every model time step by interpolating to the actual probe locations.

A number of potential deployment strategies are being studied including probe release from high-altitude balloons (Girz et al. 2002; Pankine et al. 2002), surface stations assuming positive buoyancy, and vertical profiles similar to rawinsonde measurements. Each of these deployment strategies is simulated using the ARPS/LPM on a 50-km hemispheric grid to determine long-range probe dispersion patterns. Since data impact studies are focused on much finer scales, a one-way nested grid is implemented with a grid spacing of 10 km covering a synoptic-scale domain.

[1]*Corresponding author address*: Joseph G. Dreher, ENSCO, Inc., 4849 N. Wickham Rd., Melbourne, FL 32940. e-mail: dreher.joe@ensco.com

The initial focus was on simulating probe deployment from rawinsondes at ~950 standard launch locations over the northern hemisphere. For this scenario, one probe was released every 450 m from each ascending rawinsonde beginning at 2 km above the surface and continuing through ~17 km near the top boundary of the model. The advantages of the rawinsonde deployment strategy are that it could leverage an existing observational infrastructure and allow probes to be released at a number of vertical levels over a period of 1-2 hours. A depiction of the resulting probe distribution from a June 2001 simulation over the northern hemisphere after 25 days is shown in Fig. 1a.

A strategy to deploy positively buoyant probes that ascend upward through the atmosphere was also developed. For this scenario, simulated probes are released from surface weather station sites around the northern hemisphere and ascend to a level of neutral buoyancy that depends on probe mass. This scenario examines the impact of probes remaining neutrally buoyant throughout 30-day simulations versus becoming negatively buoyant and falling out of the air gradually. A depiction of the resulting probe distribution over the northern hemisphere after 25 days is shown in Fig. 1b.

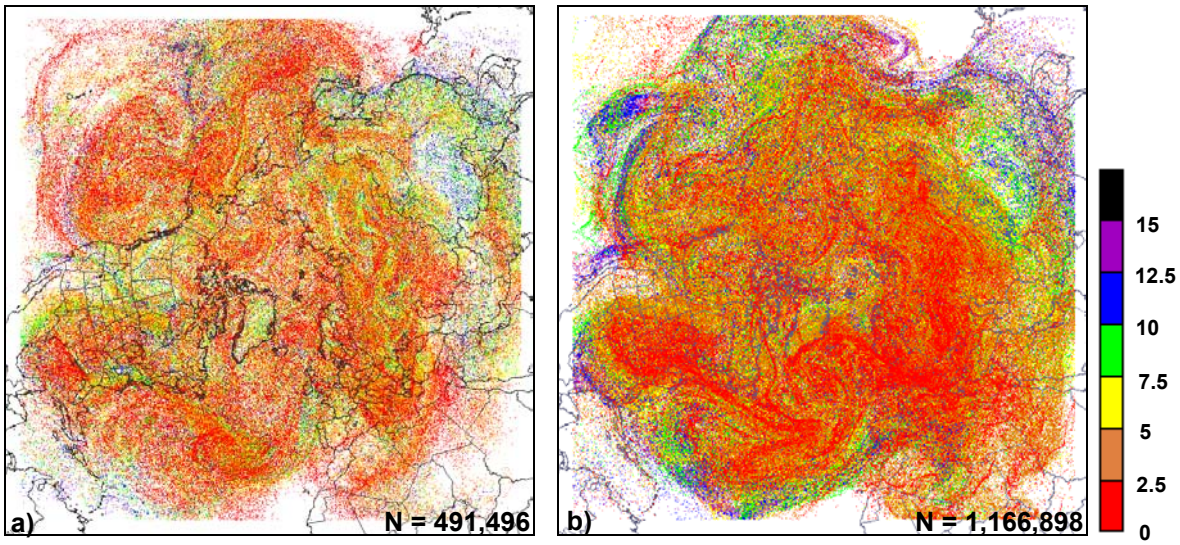

Figure 1. Probe positions for the hemispheric ARPS simulations at 0000 UTC 26 June 2001, 25 days after model initialization time for (a) rawinsonde, and (b) buoyant surface release deployment. The probe altitude (km) is denoted by the colors according to the key provided and total number of probes is given by N.

4. REGIONAL DATA IMPACT STUDY

4.1 OSSE Methodology

OSSEs are used to assess the impact of probe measurements on weather analyses and forecasts following Atlas (1997) and Lord (1997). OSSEs have been conducted for decades in meteorology to evaluate the potential impact of proposed remote and in situ observing systems, determine trade-offs in instrument design, and evaluate the most effective data assimilation (DA) methodologies to incorporate the new observations into regional and global NWP models (Arnold and Dey 1986; Rohaly and Krishnamurti 1993; Atlas 1997; De Pondeca and Zou 2001).

The model used for OSSEs is the Pennsylvania State University (PSU)/National Center for Atmospheric Research (NCAR) Fifth-generation Mesoscale Model (MM5; Grell et al. 1995). The OSSE methodology consists of three steps:

- ***Nature simulation.*** This forecast run is considered "truth", and the trajectories of all simulated probes are tracked and extracted from this model simulation. The ARPS model is used for the nature simulation.
- ***Benchmark simulation.*** The MM5 is used for the benchmark run and configured in such a manner as to generate a significantly different solution from the nature simulation to approximate the differences between a

state-of-the-art model and the real atmosphere (Atlas 1997).

- ***OSSEs.*** The various OSSEs are identical to the benchmark forecast run, except that simulated data are intermittently assimilated into MM5 at specified times.

The period of interest selected for initial study was 13-15 June 2001. During this time, a severe weather outbreak occurred over the midwest U.S. producing 72 tornadoes reported in South Dakota, Nebraska, Kansas and Iowa impacting a wide population base. The initial convective development and transition of the system from single or multicelluar structure to a well-defined squall-line feature provide an excellent opportunity to examine GEMS data impact on a regional scale.

The ARPS 50-km nature run was initialized using Aviation Model (AVN) analysis fields from 0000 UTC 1 June 2001 and run for 30 days to simulate large-scale dispersion of GEMS probes. Additional AVN analysis fields were obtained at 12-h intervals to provide lateral boundary conditions throughout the entire model run. A one-way nested 10-km domain covering a large portion of the United States was initialized at 1200 UTC 12 June 2001 and run 2 days (Fig. 2). It is important to note that all simulated observations were extracted from the 10-km domain.

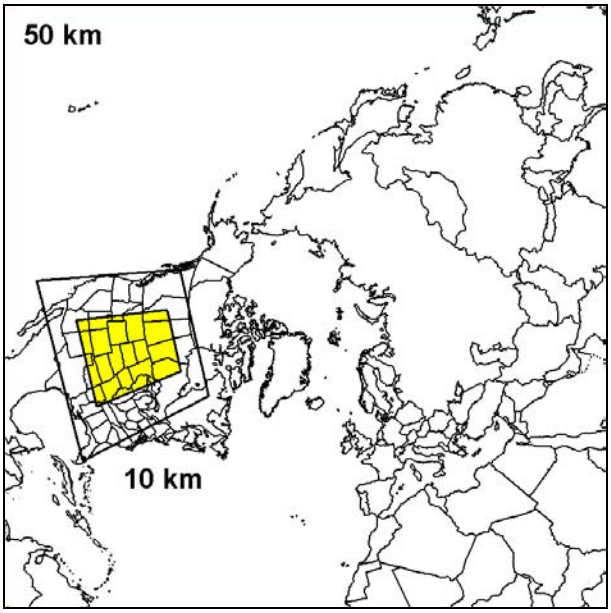

Figure 2. Domain for 50-km hemispheric ARPS simulation and coverage of 10-km grid used for regional OSSEs. Yellow-shaded box represents area of calculated objective verification statistics.

To simulate measurements obtained from probes and conventional observational networks, interpolation is used to extract values of temperature, humidity, pressure, cloud water, and other model variables at locations throughout the nature model integration. Assuming the probes are passive tracers, temporal changes in their absolute or relative position are used to estimate wind velocities. The nature run is the source of all the simulated observations and provides the truth for the OSSEs.

The MM5 benchmark simulation was initialized using the ARPS 50-km nature solution data at 0000 UTC 12 June 2001, approximately 2 days prior to the selected severe weather event. The MM5 simulation was configured with a 60-km hemispheric domain and nested 20-km domain. The MM5 20-km domain covers the same area as the ARPS 10-km domain. The benchmark run was initialized with "perfect" initial conditions by interpolating the nature solution to the benchmark grids. In addition, the same AVN hemispheric boundary conditions are used for the outermost grids of the nature and benchmark simulations.

The configuration of the OSSEs is identical to the benchmark simulation, except that simulated probe data or conventional data (surface and rawinsonde) are assimilated at select times during the model integration. Following a 24-h spin-up period, all simulated data are assimilated into the MM5 between 0000 UTC and 1200 UTC 13 June, prior to the evolution of the storm system responsible for the severe weather outbreak. A depiction of the nature, benchmark and OSSE methodology is illustrated in Fig. 3.

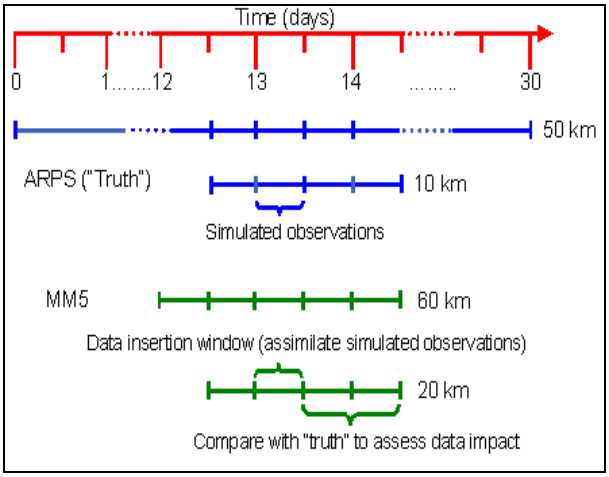

Figure 3. Summary of OSSE timeline and methodology.

Data were assimilated into the MM5 OSSEs using an intermittent DA technique similar to Rogers et al. (1996) and Manobianco (2002). This technique incorporated data from the nature run into the model integration by using the MM5 Little_r analysis package and then integrating the MM5 for a chosen time interval. The intermittent DA technique was performed at 3-h intervals during the 12-h assimilation window (Fig. 3).

Several OSSEs have been conducted thus far, and the details of each experiment are summarized in Table 1. It is important to note that all the experiments represent an upper bound to the potential forecast impact, as observations are assumed perfect with no associated error.

Table 1. Summary of simulations and OSSE experiments for 13-15 June 2001 case.

Simulation	Variables Assimilated	Experiment Description
Benchmark	N/A	No data assimilated during model integration
GEMS Rawinsonde	T,p,T_d,u,v	Data assimilated from GEMS rawinsonde deployment scenario
GEMS Surface	T,p,T_d,u,v	Data assimilated from GEMS surface deployment scenario assuming positive buoyancy
Conventional	T,p,T_d,u,v	Data assimilated from surface stations at 3-h intervals and rawinsonde sites at 0000 and 1200 UTC.

The benchmark simulation serves as a point of reference against which the OSSEs are compared, since no simulated observations were assimilated. The second and third experiments include simulated data obtained from the GEMS rawinsonde and surface deployment scenarios respectively, as explained in section 3. The assimilation method for the GEMS surface release OSSE was similar to that of the rawinsonde release experiment except simulated data were produced from the surface release scenario. Since probes remained neutrally buoyant throughout the 30-day surface release simulation versus becoming negatively buoyant and falling out of the air, probe concentrations were greater and thus average three-dimensional spacing was smaller than the rawinsonde release scenario.

The final OSSE includes data from simulated conventional networks. Simulated surface station data containing all sampled meteorological variables were assimilated into the MM5 OSSE at 3-h intervals, in a similar method to the GEMS simulated data (Table 1). In addition to the surface station data, simulated vertical sounding data were assimilated at 0000 UTC and 1200 UTC 13 June to mimic a current rawinsonde network. The ARPS 10-km nature run was the source of all simulated conventional data.

For all 20-km MM5 experiments, the 60-km MM5 simulation supplied the lateral boundary conditions. The domain was chosen as large as computationally practical to limit the influence of these pre-defined lateral boundary conditions. However, current work is in progress to investigate the importance of these boundary conditions on subsequent forecast impacts similar to the experiments performed by Weygandt et al. (2004).

Objective verification of the OSSE experiments was accomplished by calculating bias and root mean square (RMS) errors over a sub-domain centered on the event of interest (yellow-shaded box in Fig. 2) following Nutter and Manobianco (1999). If Φ represents a predicted variable from the benchmark simulation or OSSEs, then forecast error is defined as

$$\Phi' = \Phi_{\text{exp}} - \Phi_{\text{nat}}, \qquad (1)$$

where the subscripts *exp* and *nat* denote the experiment (benchmark or OSSE) and nature quantities, respectively. The bias represents the average model error of the benchmark or OSSEs, and is computed as

$$\text{Bias} = \frac{1}{\text{N}} \sum_{\text{i=1}}^{\text{N}} \Phi', \qquad (2)$$

where N represents the total number of grid points at any given height in the atmosphere. The RMS error is calculated as

$$\text{RMS Error} = \sqrt{\frac{1}{\text{N}} \sum_{\text{i=1}}^{\text{N}} (\Phi')^2}, \qquad (3)$$

For brevity, only graphs of temperature and vector wind error at 850 and 300 hPa are shown to summarize results for the OSSEs. The pressure levels were chosen to represent temperature and vector wind from the lower and upper troposphere, respectively. Results from each of the experiments are discussed in the next sub-section.

4.2 Results

4.2.1 Benchmark Simulation

Following the initialization of the MM5 20-km domain at 1200 UTC 12 June, the temperature biases and RMS errors increased with time at each level (black line in Fig. 4). The benchmark simulation indicated a cold bias, ranging from -1 to 0 K, at 850-hPa before 0000 14 June, while at 300-hPa it showed a slight warm bias ranging from 1-6 K during the entire period (Figs. 4a and c). Overall, this would indicate a stable bias in the vertical column and is noted by the lack of convective precipitation produced by the benchmark simulation when compared to the nature simulation (not shown).

The benchmark simulation also showed significant differences to the nature simulation when comparing the vector wind. The nature simulation had depicted a strong low-level jet feature at 850-hPa, whereas the benchmark simulation had no such feature. This is evident in both the bias and RMS error graphs throughout the simulation (Figs. 5a and b). The 300-hPa level winds from the benchmark run were also much weaker than the nature simulation as shown by RMS errors on the order of 15-25 m s^{-1} after 0000 13 June (Fig. 5d). The wind biases and RMS errors from the benchmark simulation are important because the absence of the strong low-level and upper-level level jets found in the nature run were likely responsible for determining the intensity and type of convective storms during the June 2001 case.

4.2.2 GEMS Rawinsonde

Following the initial assimilation of probe data at 0000 UTC 13 June, the temperature biases and RMS errors improved substantially compared to the benchmark simulation at each level (green line in Fig. 4). At 850 hPa, the benchmark simulation was too cold for a large portion of the simulation, whereas including probe data has largely corrected the bias (Fig. 4a). At 300 hPa, the benchmark simulation was too warm by 2-6 K throughout the simulation after 0000 13 June, however when including the probe data the bias dropped to near 0 K during the assimilation window and increased to near 3 K after 1200 13 June (Fig. 4b). After the data assimilation window, the 300 hPa and 850 hPa temperature RMS errors increased from approximately 1 K at 1200 UTC 13 June to 2-4 K after 0000 UTC 14 June (Figs. 4b and d).

The vector wind errors from the GEMS rawinsonde experiment were much smaller compared to the benchmark simulation for much of the period. The only exception was at 850 hPa as the RMS errors grew back by the end of the simulation (Fig. 5b) and a negative bias, at both levels, emerged by 0000 UTC 14 June (Figs. 5a and c). At 850 hPa, RMS errors decreased from near 7 m s^{-1} at 0000 UTC 13 June to near 4 m s^{-1} at 1200 UTC 13 June (Fig. 5b). At 300 hPa, RMS errors ranged from 7 m s^{-1} to 8 m s^{-1} during the data assimilation window (Fig. 5d), however, after the assimilation window the RMS errors increased from 7 m s^{-1} at 1200 UTC 13 June to 15 m s^{-1} at 1200 UTC 14 June. The reason for the increase in RMS errors and re-emergence of the negative wind bias is related to the depiction of the low-level and upper-level jet features associated with the synoptic scale low-pressure system responsible for the severe weather outbreak. The ARPS 10-km simulation still portrayed a slightly stronger flow than that of the MM5 rawinsonde experiment (not shown).

4.2.3 GEMS Surface

The graphs of temperature RMS error and bias show that the surface release experiment errors were very similar to the rawinsonde release scenario at each level (red line in Fig. 4). The only exception was during the data assimilation window at 300 hPa, where RMS errors were approximately 0.5 K less than the rawinsonde release scenario (Fig. 4d). The reason for the decrease in RMS errors in temperature during the data assimilation window is related to the probe spacing at each level for each deployment scenario. Since probes were designed to remain neutrally buoyant at different atmospheric levels the distribution was fairly well stratified with height, whereas in the rawinsonde deployment scenario the probes were designed with a terminal velocity and were stratified mainly in the lower levels of the atmosphere.

Vector wind errors show that the surface release scenario also had similar RMS errors and biases compared to the rawinsonde release experiment (red line in Fig. 5). The major

exception again was the decrease in RMS error (2-4 m s^{-1}) at 300 hPa during the assimilation window (Fig. 5d). However, the RMS error increased from near 5 m s^{-1} at 1200 UTC 13 June to near 15 m s^{-1} by 0000 UTC 14 June in both experiments (Fig. 5d).

The results from the surface release strategy suggest that the MM5 produced a very similar impact on the forecast with a significantly greater number of probes than for the rawinsonde release strategy. This is important because the experiments provide information that will be needed in the future for possible design and development of the probes and their measurement capabilities.

4.2.4 Conventional Data

Following the initial assimilation of conventional data (blue line in Figs. 4 and 5) at 0000 UTC 13 June, the temperature biases and RMS errors decreased compared to the benchmark simulation. However, it was only at the 850-hPa level that the RMS errors of temperature dropped to the similar values of the GEMS simulations (Fig. 4b). This is a result of the surface pressure being at approximately 850 hPa for a large portion of the domain. Also, at 850 hPa, the temperature RMS errors remain similar to both the GEMS simulations, ranging from 1.5-3 K after 1200 UTC 13 June (Fig. 4b).

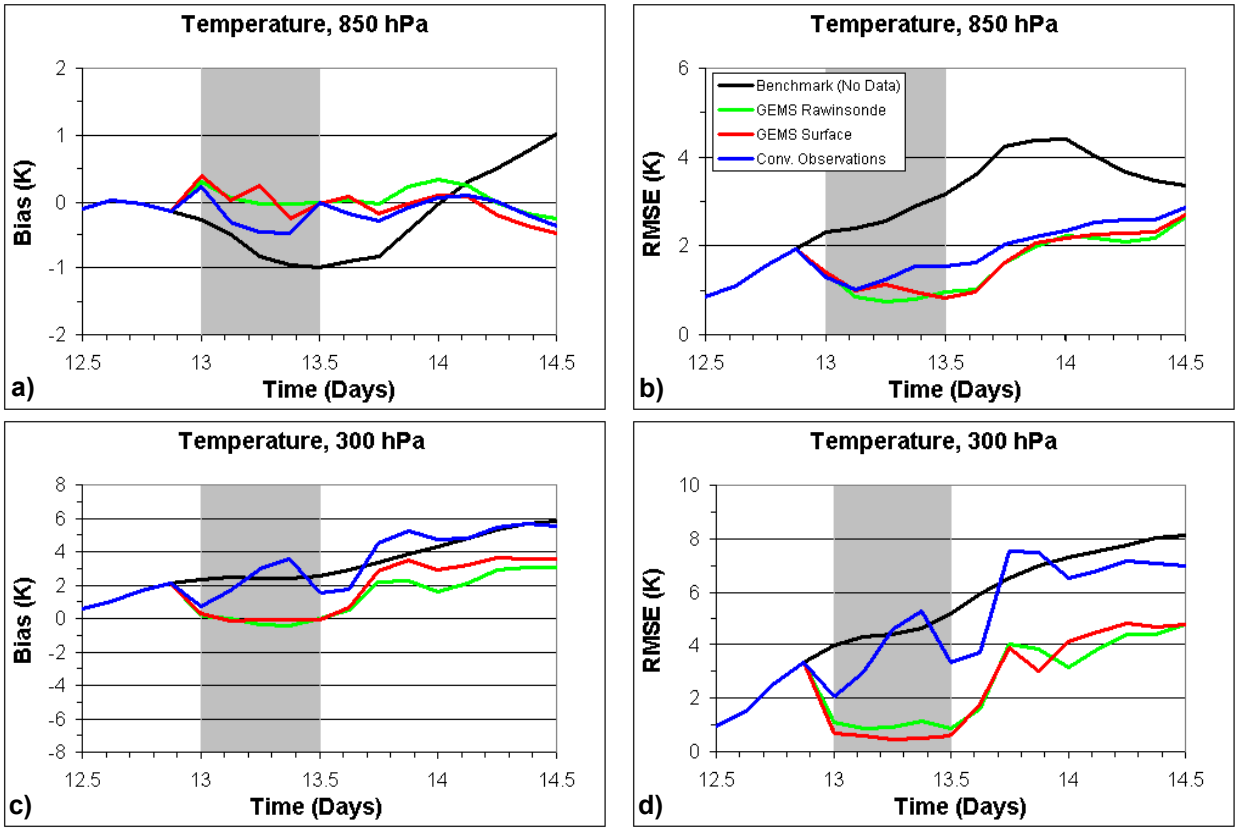

Figure 4. Graphs of temperature root mean square error (RMSE) and bias (Kelvin) for the benchmark and OSSE experiments. Data are presented for the 850- (a) and (b), and 300-hPa levels (c) and (d) for the period 1200 UTC 12 June (12.5 days) to 1200 UTC 14 June 2001 (14.5 days). The shaded area denotes the period of data insertion from 0000 to 1200 UTC 13 June 2001. Experiment type is defined by legend in panel (b).

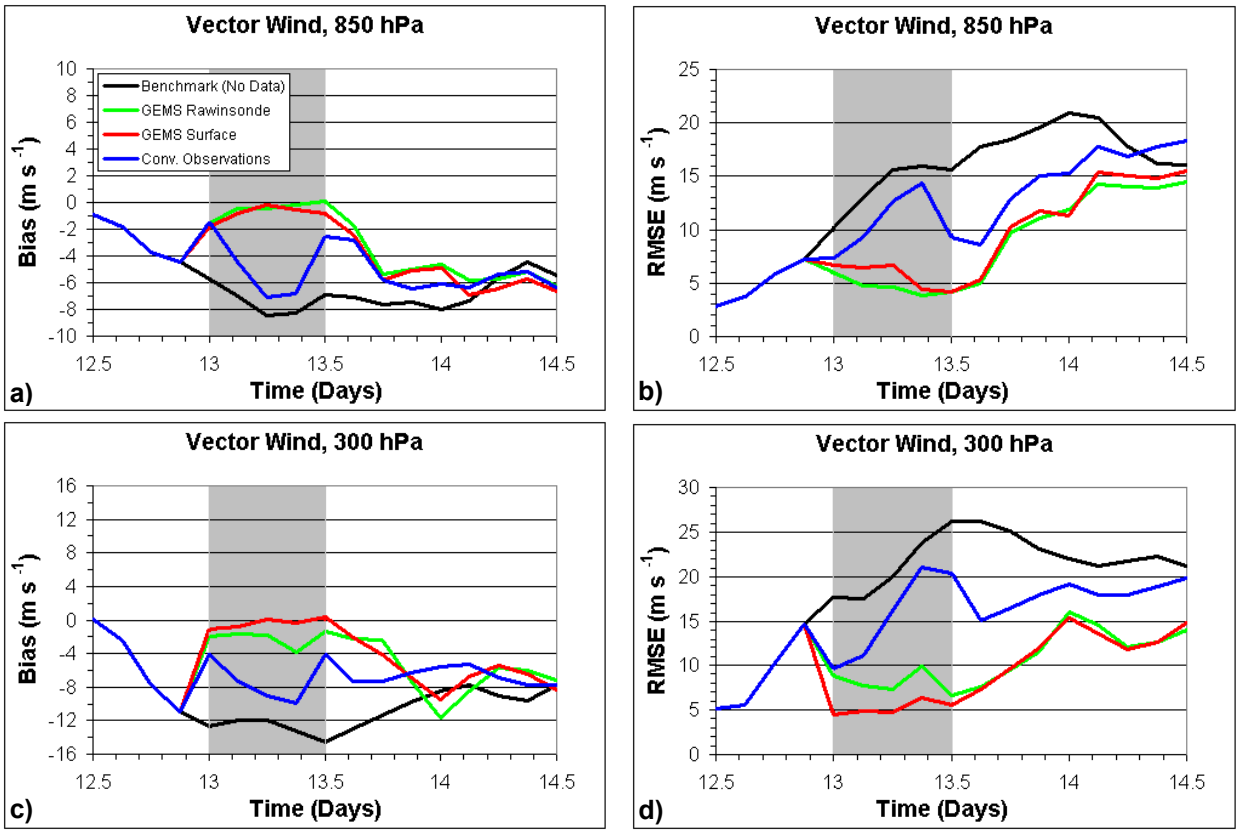

Figure 5. Graphs of the vector wind root mean square error (RMSE) and bias (m s^{-1}) for the benchmark and OSSE experiments. Data are presented for the 850- (a) and (b), and 300-hPa levels (c) and (d) for the period 1200 UTC 12 June (12.5 days) to 1200 UTC 14 June 2001 (14.5 days). The shaded area denotes the period of data insertion from 0000 to 1200 UTC 13 June 2001. Experiment type is defined by legend in panel (a).

At 300 hPa, the temperature RMS errors for the conventional simulation were 1-4 K higher than for both GEMS simulations before 1200 UTC 13 June and 2-3 K higher after 1200 UTC 13 June (Fig. 4d). The lack of vertical sounding data is apparent in the growth of temperature biases and RMS errors during the period between 0000 UTC and 1200 UTC 13 June. Meanwhile, the conventional simulation had much larger temperature RMS errors than both GEMS simulations, ranging from 3.5-7 K after 1200 UTC 13 June (Figs. 4c and d). The only exception was at 850 hPa, as the temperature RMS errors are less than 2 K from 0000 to 1800 UTC 13 June (Fig. 4b).

The vector wind errors show that the conventional simulation had smaller RMS errors and biases compared to the benchmark simulation, but larger RMS errors and biases compared to both GEMS simulations (Fig. 5). The lack of vertical sounding data is again apparent during the data assimilation window as wind vector biases and RMS errors increase with time (Figs. 5c and d). The trend after 1200 UTC 13 June indicates that the differences in errors between the conventional simulation and GEMS simulations became similar with time; however, the conventional simulation has higher biases RMS errors overall.

5. SUMMARY AND CONCLUSIONS

A set of regional OSSEs has been performed for a selected severe weather outbreak during June 2001 to evaluate the potential impact on forecasts from an ensemble of GEMS probes. Experiments were designed to evaluate the predicted impacts between several GEMS deployment scenarios and a conventional data network.

Overall, the OSSEs demonstrated that the assimilation of probe observations extracted from the ARPS nature simulation had a significant impact on improving the biases and RMS errors of several predicted primary variables over the MM5 benchmark simulation. On the other hand,

assimilation of simulated conventional data yielded less of an impact on the forecasted values especially at non-rawinsonde release times.

Based on the results obtained from these preliminary OSSEs, further work dealing with GEMS simulated probes is required. Experiments are underway to examine:

- Sensitivity to deployment scenario, precipitation scavenging, data density, and data assimilation period and frequency.
- OSSE depiction of the evolution of the case from single or multicelluar storm structure to a well-defined squall-line feature compared to the nature simulation.
- Realistic errors added to the assimilated meteorological variables.
- Importance of the current pre-defined lateral boundary conditions on the forecast impact especially at times after data assimilation.
- Calibration of simulated conventional observations by comparing impact to assimilating real observations.
- Additional OSSEs including a chosen winter case, longer time periods, and forecast cycles similar to Weygandt et al (2004).

6. ACKNOWLEDGEMENTS

This work was supported by the Universities Space Research Association's NASA Institute for Advanced Concepts.

7. REFERENCES

Arnold, C. P. Jr., and C. H. Dey, 1986: Observing system simulation experiments: Past, present, and future. *Bull. Amer. Meteor. Soc*., **67**, 687-695.

Atlas, R., 1997: Atmospheric observations and experiments to assess their usefulness in data assimilation. *J. Royal Meteor. Soc. Japan*, **75**, 111-130.

Brewster, K., 1996: Application of a Bratseth analysis scheme including Doppler radar data. Preprints, *15th Conf. on Weather Analysis and Forecasting*, Amer. Meteor. Soc., Norfolk, VA, 92-95.

De Pondeca, M. S. F. V., and X. Zou, 2001: Moisture retrievals from simulated zenith delay "observations" and their impact on short-range precipitation forecasts. *Tellus,* **33A**, 192-214.

Deardorff, J. W., 1980: Stratocumulus-capped mixed layers derived from a three-dimensional model. *Bound.-Layer Meteor*., **7**, 199-226.

Girz, C. M. I. R, and Coauthors, 2002: Results of the demonstration flight of the GAINS prototype III balloon. Preprints, *6th Symp. On Integrated Observing Systems*, Amer. Meteor. Soc., Orlando, FL, 248-253.

Grell, G., J. Dudhia, and D. Satuffer, 1995: A description of the Fifth-Generation Penn State/NCAR mesoscale model (MM5). NCAR / TN-398 + STR [Available on line at http://www .mmm.ucar.edu/mm5/mm5-home.html].

Holland, G. J., and Coauthors, 2001: The aerosonde robotic aircraft: A new paradigm for environmental observations. *Bull. Amer. Meteor. Soc*., **82**, 889-901. (not cited in text)

Lord, S. J., E. Kalnay, R. Daley, G. D. Emmitt, and R. Atlas, 1997: Using OSSEs in the design of the future generation of integrated observing systems. Preprints, *First Symposium on Integrated Observing Systems*, Amer. Meteor. Soc., Long Beach, CA, 45-47.

Manobianco, J., 2002: Global Environmental MEMS Sensors (GEMS): A Revolutionary Observing System for the 21st Century, Phase I Final Report. [Available online at http://www.niac. usra.edu/studies/].

Nutter, P. A., and J. Manobianco, 1999: Evaluation of the 29-km Eta model. Part I: Objective verification at three selected stations. *Wea. Forecasting*, **14,** 5-17.

Mellor, G. L., and T. Yamada, 1982: Development of a turbulence closure model for geophysical fluid problems. *Rev. Geophys. Space Phys*., **20**, 851-875.

Pankine, A. A., E. Weinstock, M. K. Heun, and K. T. Nock, 2002: In-situ science from global networks of stratospheric satellites. Preprints, *6th Symp. On Integrated Observing Systems*, Amer. Meteor. Soc., Orlando, FL, 260-266.

Rogers, E., T. L. Black, D. G. Deaven, G. J. DiMego, Q. Zhao, M. Baldwin, N. W. Junker, and Y. Lin, 1996: Changes to the operational "early" eta analysis/forecast system at the National Centers for Environmental Prediction. *Wea. Forecasting,* **11,** 391-413.

Rohaly, G. D., and T. N. Krishnamurti, 1993: An observing system simulation experiment for the Laser Atmospheric Wind Sounder (LAWS). *J. Applied Meteor.*, **32**, 1453-1471.

Seinfeld, J. H., and S. N. Pandis, 1998: *Atmospheric Chemistry and Physics – From Air Pollution to Climate Change*, John Wiley and Sons Inc., New York, 1326 pp.

Weygandt, S.S., and coauthors, 2004: Potential forecast impacts from space-based lidar winds: Regional observing system simulation experiments. *8thSymp. Int. Obs. and Assim. Systems for Atm. Oceans and Land Surf.,* Seattle, Amer. Meteor. Soc.

Xue, M., K. K. Droegemeier, and V. Wong, 2000: The Advanced Regional Prediction System (ARPS) — A multi-scale nonhydrostatic atmospheric simulation and prediction model. Part I: Model dynamics and verification. *Meteor. Atmos. Phys.*, **75**, 161-193.

_____, and Coauthors, 2001: The Advanced Regional Prediction System (ARPS) — A multiscale nonhydrostatic atmospheric simulation and prediction tool. Part II: Model physics and applications. *Meteor. Atmos. Phys.*, **76**, 143-165.